Hindawi
Structural Control and Health Monitoring
Volume 2023, Article ID 8128701, 13 pages
https://doi.org/10.1155/2023/8128701

WILEY | Hindawi

Research Article

A Novel Back-Analysis Approach for the External Loads on Shield Tunnel Lining in Service Based on Monitored Deformation

Wei Lin, Pan Li, Xiongyao Xie, Yuyang Cao, and Yangbin Zhang

Department of Geotechnical Engineering, College of Civil Engineering, Tongji University, Shanghai 200092, China

Correspondence should be addressed to Pan Li; yongpanli@163.com

Received 10 December 2022; Revised 5 March 2023; Accepted 20 June 2023; Published 27 June 2023

Academic Editor: Yi-Qing Ni

The maintenance of in-service shield tunnel lining has become a critical issue in recent decades due to the rapid development of the metro system in China. The external load is one of the most important factors influencing the deformation and performance of the in-service shield tunnels. It is hard to evaluate the external load since it is influenced by complex factors. And the arbitrary-distributed external load is not considered in the existing theories. A novel back-analysis approach for evaluating the external load using the deformation of tunnel lining was proposed based on Betti's theorem. The theoretical rationality of the proposed method is analyzed, and the workflow is provided. The data and simulation models for a model test were adopted to validate the effectiveness and accuracy of the proposed method. The results show that the external loads can be back-analyzed with satisfying accuracy and low computational cost. Then, the practical application was conducted for an in-service shield tunnel. In addition, the workflow combined with laser scanning and back analysis was proposed for evaluating the practical loads. The proposed approach can be used for the back analysis of the external loads based on lining deformation scanned inside tunnels, with good performance.

1. Introduction

The intense urbanization demands the large development of underground infrastructure. The utility tunnels in urban areas, taking metro tunnels as examples, are mainly constructed by shield machines given the soil ground conditions. With the huge construction of metro tunnels, the maintenance of in-service shield tunnels has become a critical concern for the regions with soil ground. Existing and potential defects will reduce the performance of in-service shield tunnels [1, 2]. Load condition is critical for evaluating the structural performance of shield tunnels when considering the maintenance scheme of the shield tunnel structure [3, 4].

According to previous research on the structural performance of shield tunnels [2, 5, 6], the load-structure method is widely employed for the evaluation of shield tunnels, where different load-distribution patterns such as linear patterns and parabolic patterns are adopted. Furthermore, the stratum-structure method is used to calculate the loads on the lining structure [7, 8], in which the interaction between the surrounding ground and structure is taken as the external load on the lining. During the operational phase of shield tunnels, the load on the lining is generally influenced by multiple factors, including adjacent construction [9, 10], surcharge load [11], vehicle vibration [12, 13], and long-term water leakage [14]. These uncertain factors during service will result in structural deformation in both longitudinal and transverse directions [15, 16]. However, the load-structure method and stratum-structure method are limited when considering the variation of the load distribution on the lining structure [17, 18]. Hence, the load models for both the load-structure method and stratum-structure method should be updated when evaluating the performance of in-service shield tunnels. While in most cases, it is not feasible to obtain the external loads of shield tunnels by using either pressure gauges or the classic earth pressure formulas [18].

Back analysis is considered an effective approach for determining unknown parameters in geotechnical engineering [19–21]. For the external loads on the shield tunnel lining, the back-analysis methods can be classified into two

types, namely strain-based and deformation-based methods. The strain-based methods are widely used for the estimation of external loads during tunnelling, with promising accuracy [22] while the strain of the lining will be required as the input, which is costly and hard to be collected for shield tunnels in service. Hence, the application of strain-based methods on the in-service shield tunnels is not practical [23, 24]. The deformation-based methods provide feasible perspectives for in-service shield tunnels, given the accessibility of deformation monitoring. The existing deformation-based methods are mainly proposed and applied for rock tunnels [25], the structures of which are quite different from shield tunnels. The property and in-situ stress of surrounding rock can be estimated by performing back analysis of matching numerical modelling results with the measured tunnel convergence [26, 27]. Furthermore, the long-term creep and water effects on rock tunnel lining can be back-analyzed based on deformation [28]. It is noted that most of the existing back-analyzed parameters are generalized, heavily dependent on the selected theoretical models, and affected by limited or incomplete monitoring data [29–31]. As for the back analysis of external loads, full-ring load distribution is not taken into consideration in related research currently [18, 32–34]. In general, the application of deformation-based methods on shield tunnel loads remains to be solved, also due to the difficulty in the interpretation of deformation patterns [35]. Recently, meta-model methods based on numerical simulation have been applied in the back analysis of tunnel engineering [36–38], where complex optimization algorithms with expensive computational costs are required. The load distribution on the shield tunnel lining in service is rarely investigated due to the limitations of the existing methods.

In this work, the back-analysis method for the external load on the lining structure in service is investigated from the perspective of Betti's theorem. The physical models required in Betti's theorem can be replaced by the corresponding numerical models. Then, a novel back-analysis approach is proposed to calculate the load on tunnel lining in the operational phase based on Betti's theorem and small-strain assumption. This paper is composed of the following 5 parts: (1) the principle and the relation between Betti's theorem, i.e., Maxwell–Betti reciprocal work theorem, and the proposed back-analysis approach are illustrated; (2) the loads on the shield tunnel lining in service were analyzed by conventional load-structure models and scanned deformation; (3) the back-analysis approach was proposed based on Betti's theorem and the load-structure model; (4) the feasibility of the proposed approach was investigated theoretically; (5) the proposed back-analysis approach was verified by comparison with the model test results and applied for practical engineering.

2. Methodology

2.1. Betti's Theorem. Betti's theorem is one of the laws used for structural analysis [39]. The deformation is one of the most important parameters for structural analysis. And Betti's theorem is widely used in the deformation calculation of structures in the design phase [40]. The energy from external forces will be transformed into the strain energy of the elastic body according to the Law of Conservation of Energy. This principle can be employed for calculating the stress and strain of the deformable body subjected to external loads. It is usually assumed that other kinds of energy losses (e.g., acoustic energy and thermal energy) are small enough to be ignored during the deformation of the elastic body.

As shown in Figure 1, if an elastic body is subjected to a set of external forces, i.e., the body force (f_x, f_y, f_z) and surface force (q_x, q_y, q_z), the strain can be expressed in the Cartesian coordinate system as follows:

$$\left.\begin{aligned} &\varepsilon_x = \frac{\partial \delta_x}{\partial x}, \varepsilon_y = \frac{\partial \delta_y}{\partial y}, \varepsilon_z = \frac{\partial \delta_z}{\partial z}, \\ &\gamma_{xy} = \frac{\partial \delta_x}{\partial y} + \frac{\partial \delta_y}{\partial x}, \gamma_{yz} = \frac{\partial \delta_z}{\partial y} + \frac{\partial \delta_y}{\partial z}, \gamma_{xz} = \frac{\partial \delta_x}{\partial z} + \frac{\partial \delta_z}{\partial x} \end{aligned}\right\}, \tag{1}$$

where δ_x, δ_y, and δ_z are the displacement caused by the external forces along the three Cartesian coordinate orientations, ε_x, ε_y, and ε_z are the three normal strains in the elastic body, and γ_{xy}, γ_{yz}, and γ_{xz} are the three shear strains.

For the second set of external forces, as illustrated in Figure 1, the induced strain by these forces can be expressed as follows:

$$\left.\begin{aligned} &\varepsilon_x' = \frac{\partial \delta_x'}{\partial x}, \varepsilon_y' = \frac{\partial \delta_y'}{\partial y}, \varepsilon_z' = \frac{\partial \delta_z'}{\partial z}, \\ &\gamma_{xy}' = \frac{\partial \delta_x'}{\partial y} + \frac{\partial \delta_y'}{\partial x}, \gamma_{yz}' = \frac{\partial \delta_z'}{\partial y} + \frac{\partial \delta_y'}{\partial z}, \gamma_{xz}' = \frac{\partial \delta_x'}{\partial z} + \frac{\partial \delta_z'}{\partial x} \end{aligned}\right\}, \tag{2}$$

where $(\varepsilon_x', \varepsilon_y', \varepsilon_z')$ and $(\gamma_{xy}', \gamma_{yz}', \gamma_{xz}')$ are the normal and shear strains induced by the set of external forces (f_x', f_y', f_z') and (q_x', q_y', q_z'), respectively.

The energy (ε_{12}) from the first set of forces associated with the deformation caused by the second set of forces can be expressed as follows:

$$\varepsilon_{12} = \iiint_\tau \left[\left(f_x - \rho\frac{\partial^2 \delta_x}{\partial t^2}\right)\delta_x' + \left(f_y - \rho\frac{\partial^2 \delta_y}{\partial t^2}\right)\delta_y' + \left(f_z - \rho\frac{\partial^2 \delta_z}{\partial t^2}\right)\delta_z'\right]dV + \iint_S \left(q_x\delta_x' + q_y\delta_y' + q_z\delta_z'\right)dS. \tag{3}$$

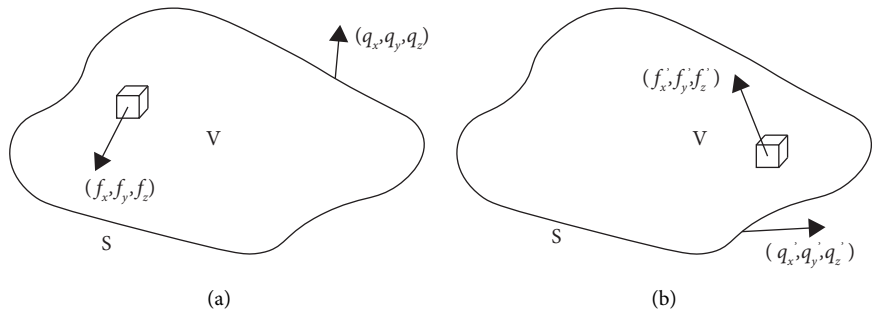

Figure 1: An elastic body subjected to two sets of external forces, including both body forces and surface forces: (a) the illustration of the first set of external forces and (b) the illustration of the second set of external forces.

Likewise, the energy (ε_{21}) from the first set of forces associated with the deformation caused by the second set of forces can be expressed as follows:

$$\varepsilon_{21} = \iiint_{\tau}\left[\left(f_x' - \rho\frac{\partial^2\delta_x'}{\partial t^2}\right)\delta_x + \left(f_y' - \rho\frac{\partial^2\delta_y'}{\partial t^2}\right)\delta_y + \left(f_z' - \rho\frac{\partial^2\delta_z'}{\partial t^2}\right)\delta_z\right]dV + \iint_{S}\left(q_x'\delta_x + q_y'\delta_y + q_z'\delta_z\right)dS. \tag{4}$$

According to Betti's theorem, the following work balance equation is obtained:

$$\varepsilon_{12} = \varepsilon_{21}. \tag{5}$$

Without considering the body inertia forces, the following expression is obtained:

$$\int_S q_i\delta_i' dS = \int_S q_i'\delta_i dS. \tag{6}$$

This matrix-form equation can be written as follows:

$$[q]_n\left[\delta'\right]_n = \left[q'\right]_n[\delta]_n. \tag{7}$$

It can be seen from equation (7) that either set of external forces can be determined based on another three items in the equation if the three items are provided. The property of the theorem enables the determination of loads based on the measured deformation [41, 42]. Hence, the theorem can be applied in the health monitoring of shield tunnels to solve the challenges induced by the uncertainty of the changing load conditions during service. The illustrated derivation process is restricted to the background of linear-elastic material while Betti's theorem has been expanded to more generalized backgrounds [43], including elastic-plastic material, which is the main constitutive model applied in tunnel engineering.

2.2. The Load-Deformation Model. The shield tunnel lining is positioned underground by shield machines. A ring of tunnel lining is a cylindrical structure assembled by prefabricated segments. One of the most widely adopted load patterns of the tunnel lining during construction is illustrated in Figure 2. The external loads acting on the tunnel lining are usually assumed to be linearly or quadratically distributed around the shield tunnel lining [34], including the vertical pressure at the tunnel crown, the horizontal ground pressure, and the ground reaction at the tunnel bottom. However, the distribution modes of external load on the lining in service are usually way more complex than the simplified assumption.

The laser scanning data of lining rings with typical deformation in a metro line are displayed in Figure 3, denoted as Example I, Example II, and Example III, where the deformation is scaled 10 times for demonstration. The arbitrary and random patterns of lining deformation can be found. Furthermore, the location distribution of the maximum convergence involving successive 1100 lining rings is provided in Figure 4, where the uncertainty of deformation induced by various load patterns is displayed clearly. It is noted that only the ring-wise deformation is discussed here. The variation of deformation patterns may be greater if the segment-wise deformation is taken into consideration. The lining ring deformation is dominated by stochasticity due to the unclear pressure of soil and water. According to the conventional assumption depicted in Figure 2, the deformation patterns should be symmetric and similar to each other while it can be observed that the deformation patterns of the shield tunnel lining rings in service are irregular and different from each other. Hence, it is unreasonable if the conventional assumption is used for mechanical analysis of the life-cycle performance. It is found that the lining ring of shield tunnels may be subjected to eccentric or irregular load patterns during service due to various factors [44, 45], including water leakage, vehicle vibration, adjacent excavation, and surface loading. It is indicated that the description of the load patterns should cover different cases.

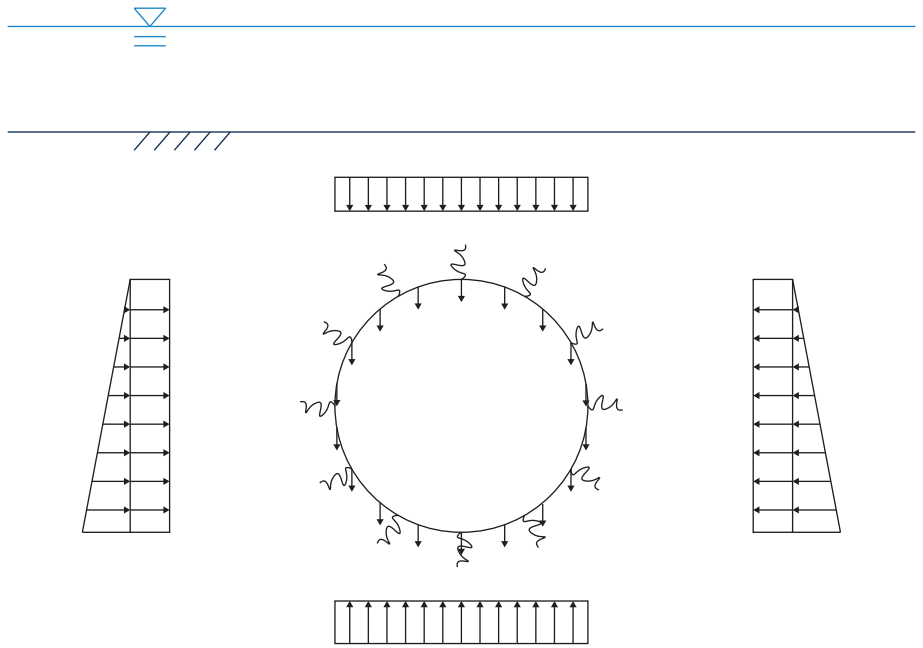

Figure 2: The external load pattern on the lining structure during the construction phase.

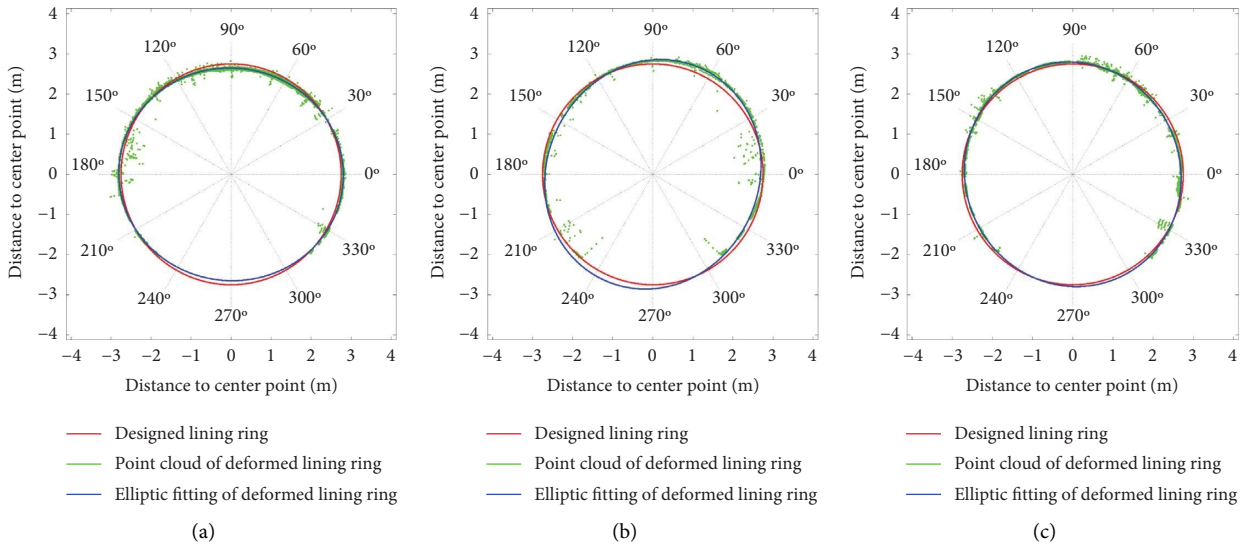

Figure 3: The deformation of lining rings scanned in a metro line: (a) example I; (b) example II; (c) example III.

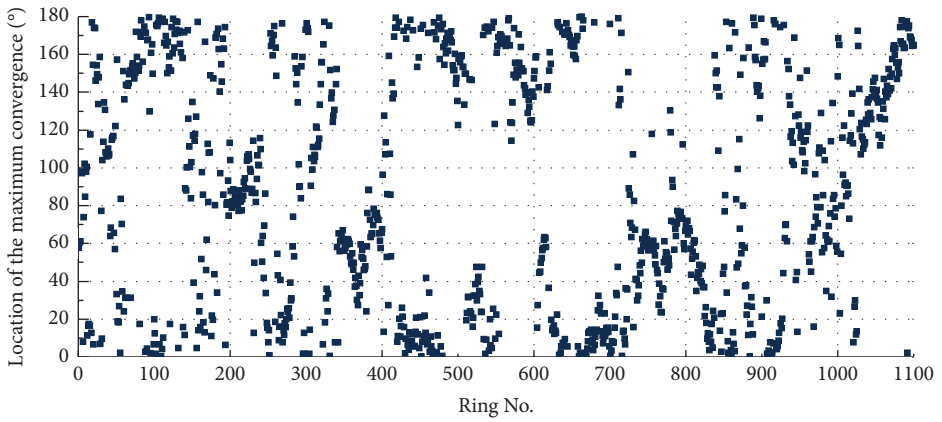

Figure 4: The location distribution of the maximum lining ring convergence in a metro line.

2.3. The Back-Analysis Model for External Loads. As plotted in Figure 5(a), the arbitrarily distributed ground-structure interaction on the shield tunnel lining can be simplified as a series of loads distributed around the tunnel lining (denoted as $\{x_i\}(i = 1, 2, \ldots, n)$), where x_i denotes the external load on the lining. The corresponding structural deformation is denoted by $w_i(i = 1, 2, \ldots, n)$. The set of loads is denoted as Load Case I. And the lining ring is assumed to be subjected to another designed set of loads $\{F_i\}(i = 1, 2, \ldots, n)$, denoted as Load Case II and shown in Figure 5(b), with corresponding structural deformation $v_i(i = 1, 2, \ldots, n)$. Load Case I is the real load condition on the structures, and Load Case II is an assumed load condition. The loads in both load cases can be generalized loads, including distributed force, concentrated force, and moment. The distribution of the loading positions in Load Case II depends on the deformation measuring points.

According to Betti's theorem, if the material of the tunnel lining is linear elastic, the following equation between Case I and Case II can be obtained:

$$\{v_n\} \cdot \{x_n\} = \{f_n\} \cdot \{w_n\}, \tag{8}$$

where $\{v_n\}$ is the structural deformation along the direction of $\{x_n\}$ in Load Case II (subjecting to the load set $\{f_n\}$). Likewise, $\{w_n\}$ is the lining deformation along the direction of $\{f_n\}$ in Load Case I (subjecting to the load set $\{x_n\}$).

As shown in equation (8), the load set $\{x_n\}$ can be calculated based on the other three items, i.e., $\{f_n\}$, $\{v_n\}$, and $\{w_n\}$. In order to solve the unknown load set $\{x_n\}$, a total number of n load cases should be created first, which constitutes the equation set shown as follows:

$$[V]_{n\times n} \cdot [X]_{n\times 1} = [F]_{n\times n} \cdot [W]_{n\times 1}, \tag{9}$$

where $[F]_{n\times n}$ denotes the external load matrix of Load Case II, $[V]_{n\times n}$ denotes the corresponding structural deformation matrix, $[X]_{n\times 1}$ denotes the matrix of the external load of Load Case I, and $[W]_{n\times 1}$ denotes the corresponding structural deformation matrix. It is noted that the $[F]_{n\times n}$ is a diagonal matrix made up of $\{f_n\}$.

In practice, the deformation matrix $[W]_{n\times 1}$ can be measured by laser scanning as displayed in Figure 4. Varieties of methods and corresponding instruments have been proposed for deformation measurement in shield tunnels, such as total station, laser convergence gauge, tilt sensor, and optical-fibre sensors [46]. However, the deformation derived by the above methods is incomplete. These methods are designed for isolated measuring points and usually rely on instruments installed on the lining while the development of laser scanning technology enables the efficient acquisition of large point cloud data during the life cycle of shield tunnels [16], in which detailed three-dimensional space information is included. The accuracy of deformation measurement based on laser scanning is proved to archive the submillimetre level with proper data processing [47]. The full-ring deformation can be measured based on the point cloud data by the following steps, including preprocessing the point cloud, extracting the tunnel axis, performing the coordinate transformation, performing noise reduction, and fitting the deformation [48]. The automatic workflow of the steps has also been developed [49]. It is indicated that the application of laser scanning in deformation measurement has the advantages of comprehensiveness and efficiency [16].

The load set $[F]_{n\times n}$ and the corresponding structural deformation $[V]_{n\times n}$ can be obtained by numerical analysis for the same tunnel lining. Thus, the actual external load $[X]_{n\times 1}$ based on the measured deformation $[W]_{n\times 1}$ can be calculated based on equation (9) by substituting $[W]_{n\times 1}$, $[F]_{n\times n}$, and $[V]_{n\times n}$.

The overall workflow of the back-analysis method is demonstrated in Figure 6. In general, there are two main steps in the back analysis of the external load on the tunnel lining during service. The first main step is to build and calculate the numerical model of the prototype shield tunnel lining. Then, the back analysis can be carried out by the equations derived from equation (9) while it is noted that the existence and uniqueness of the solution should be investigated before further study.

2.4. Existence and Uniqueness of the Solution. Segments of shield tunnels are assembled by steel bolts, which form the joints between segments. Although the mechanical behaviour of joints may be nonlinear and complex, it is indicated that the connecting bolts can be regarded as a linear-elastic material under the small-strain condition [50]. In general, the material of the lining rings can also be assumed to be linear elastic under the small-strain condition [51]. The proposed back-analysis approach can be used for determining the external load on the shield tunnel lining since the requirements of applying Betti's Theorem are satisfied.

For a nonhomogeneous linear equation $Ax = b$, the uniqueness of the solution is required, which means that the matrix A will be full rank and can be expressed as follows:

$$r(A, b) = r(A) = A. \tag{10}$$

The matrix A is built by n groups of load cases. Thus, the rationality of the load cases constructed in numerical simulations is of great importance. If the load cases are not rational, the matrix might be ill-posed which results in an incorrect solution [52]. The linear equation sets are solved by the singular value decomposition method using MATLAB in this work.

3. Validation and Application

3.1. Physical Model. The external load on tunnel lining is hard to monitor during service due to the low durability of pressure sensors. Therefore, a full-scale model test on the lining structure [53] is employed to verify the accuracy and feasibility of the proposed back-analysis method. As shown in Figure 7, a single-layer tunnel lining with a thickness of 0.48 m and a width of 1.50 m is adopted in the model test, which is cast with concrete C55. The outer diameter of the lining ring is 6.80 m. Segments are connected by bolts of M36 steel, of which the positions are shown in Figure 7. The segments are fixed to steel support at the end and are subjected to the vertical load P and the horizontal load N.

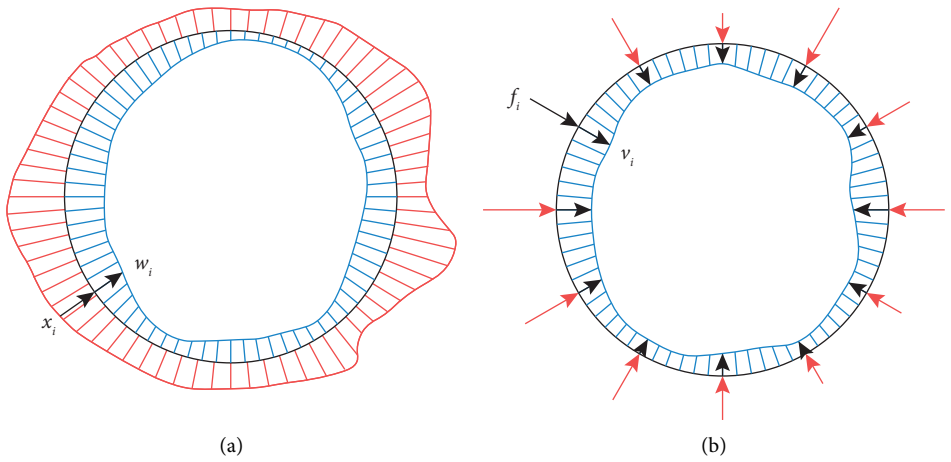

Figure 5: The load-deformation model: (a) Load Case I; (b) Load Case II.

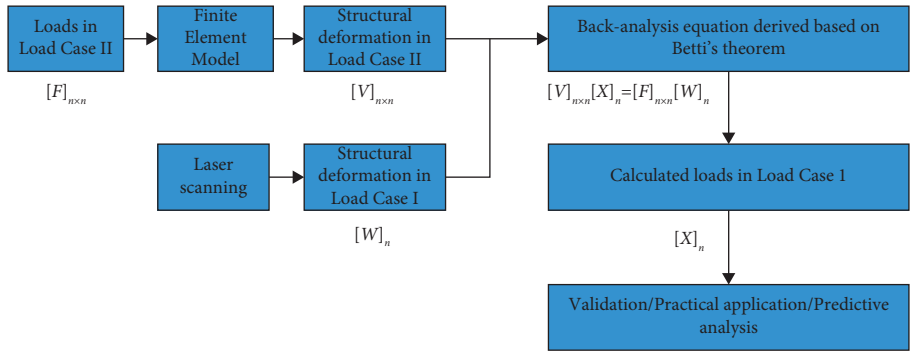

Figure 6: The workflow of the proposed back-analysis method.

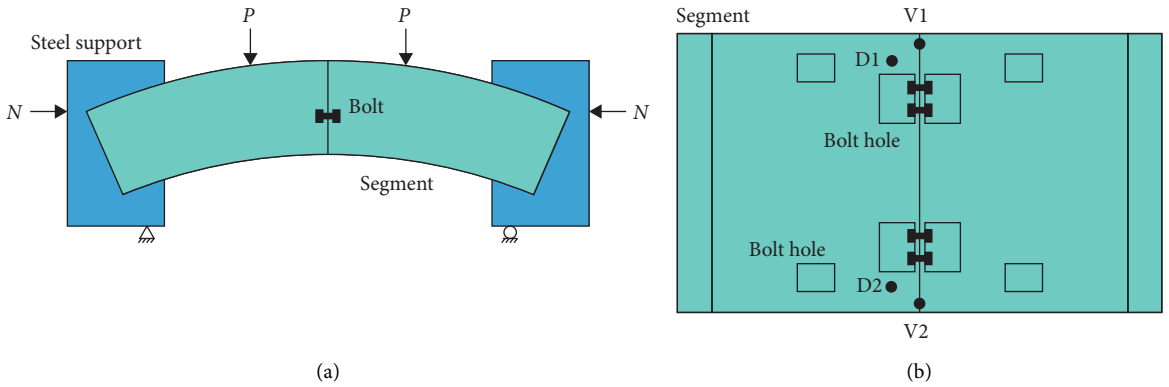

Figure 7: The schematic of the model test [53]: (a) the main view and (b) the side view.

The vertical load was given by vertical hydraulic jacks through a set of stiff steel distribution beams. At the end of the tunnel segment specimen, the horizontal load was provided by hydraulic jacks. The mechanical behaviours of segments under the effect of both positive and negative bending moments were investigated in the model test. The direction of vertical load P in the case of positive bending moment was downward and was upward otherwise.

The positions of deformation measuring points are also marked in Figure 7. The vertical displacement of the segments was measured using two vertical displacement sensors D1 and D2. The deformation of joints at both the external side and internal side was recorded by a pair of displacement transducers V1 and V2.

3.2. Numerical Model. For the proposed approach, the numerical model is required for building the equations to calculate the actual external load on the shield tunnel lining. The physical model is adopted as the prototype of the numerical model. The finite element software ANSYS10.0 is employed to carry out the 3D mechanical

analysis. The idea of simulation adopted is based on the strip method. The parts of the finite element model for further analysis are shown in Figure 8, corresponding to the model test illustrated in Figure 7. The joint with a width of 110 mm is modelled by the material with the reduced Young's modulus. The friction between the surfaces of concrete is not considered in the simulation for lower computational cost. The shear force on the joint is assumed to be mainly undertaken by the connecting bolts, of which the rationality has been proved [54]. The connecting bolts were modelled according to the actual length, with both ends fixed. The element solid65 and element beam188 are used for lining segments and connecting bolts, respectively. The mechanical properties of different materials in the finite element model are demonstrated in Table 1.

To verify the rationality of the numerical model, the vertical displacement and joint opening of the specimens are compared with the results of the model test, displayed in Figure 9. For the same value of loads in the model test, the greatest value of deformation is selected for comparison. The test data in the unloading phase are not considered since the purpose of this work is not to investigate elaborated models. It can be found that the simulation results fit the model test well, especially in the phase of small loads. It is indicated that the numerical model is rational to be used for the back analysis of the external loads on the specimens of the full-scale model test.

3.3. Back Analysis of the Model Test. The external loads on the segment specimens in the model test are denoted as Load Case I, i.e., $[X_i]_{4\times1}(i = 1, 2, 3, 4)$, where X_1, X_2 is equal to the vertical load P and X_3, X_4 is equal to horizontal load N. The corresponding displacement at the loading position is denoted as $[W_i]_{4\times1}(i = 1, 2, 3, 4)$, which was calculated geometrically based on the monitored deformation in the model test.

Based on the physical model, the numerical model was created to calculate the deformation under the effect of Load Case II $[F_{ij}]_{4\times4}(i, j = 1, 2, 3, 4)$, where F_{ii} denotes the assumed load, and other elements are equal to 0. The loads are assumed to act at the position of measuring points D1, D2, V1, and V2, including concentrated force and concentrated moment. The corresponding deformation calculated in the numerical model is denoted as $[V_{ij}]_{4\times4}(i, j = 1, 2, 3, 4)$, where V_{ij} is the displacement at the position of the j-th load of Load Case I induced by the i-th load of Load Case II. Then, the back-analysis equations based on Betti's theorem can be expressed as follows:

$$[X_i]_{4\times1} = \left[V_{ij}\right]^{-1}_{4\times4} \cdot \left[F_{ij}\right]_{4\times4} \cdot [W_i]_{4\times1}. \tag{11}$$

There were 50 sets of data collected in the loading phase of the model test, which were adopted for validation. The comparison between the back-analysis results and the loads monitored in the model test is presented in Figure 10. In general, the back-analysis results achieved promising accuracy for both vertical and horizontal loads. The average errors are 76.01 kN for vertical loads and 50.55 kN for horizontal loads. The errors may become greater with larger loads, which is similar to the errors of the numerical simulation shown in Figure 9. The back-analysis errors are acceptable given that the numerical simulation was performed based on the assumption of small deformation and elastic materials. It is indicated that the proposed back-analysis approach can be used for calculating the external loads on the lining structure.

3.4. Practical Application. The numerical simulation models for the practical application were built to carry out the full-ring mechanical analysis, displayed in Figure 11. The concrete segment, steel reinforcement, joints, and connecting bolts are all considered in the simulation model. The two load cases adopted here are the same as illustrated in Figure 5. The number of loads in the load cases, which is 6 here, depends on the demands of mechanical analysis. For both Load Case I and Load Case II, the 6 loads are designed at the centre of each segment. The full-ring load value can be calculated via spline interpolation. With the simulation results, the equation for the back analysis of load on the lining can be derived from equation (9), written as follows:

$$\begin{bmatrix} q_1 \\ q_2 \\ q_3 \\ q_4 \\ q_5 \\ q_6 \end{bmatrix} = \begin{bmatrix} 31623548 & 13552500 & 14369386 & 15474930 & 24255507 & 23008400 \\ 18541972 & 35913554 & 253141 & 28105279 & 20528024 & 35212454 \\ 43922647 & -24901211 & 76929016 & -24920394 & 43995894 & 6909980 \\ 20409642 & 28022979 & 178471 & 35844835 & 18369821 & 35092852 \\ 24348727 & 15534303 & 14424466 & 13604229 & 31744396 & 23096624 \\ 21369146 & 25606141 & 6371605 & 25606746 & 21366300 & 40048730 \end{bmatrix} \begin{bmatrix} \delta_1 \\ \delta_2 \\ \delta_3 \\ \delta_4 \\ \delta_5 \\ \delta_6 \end{bmatrix}. \tag{12}$$

The point clouds of 3 lining rings, namely Ring I, Ring II, and Ring III, in a shield tunnel project, were selected for the demonstration of the practical application. The deformation of the selected lining rings is plotted in Figure 12, of which the maximum convergence is around 0.5%, 1.0%, and 1.5% of the 6.2 m outer diameter, respectively. It is noted that the deformation in Figure 12 is scaled 10 times for easier understanding. With the scanned deformation as the input, the loads on the lining can be calculated by equation (9). The back-analysis results of the loads with spline interpolation

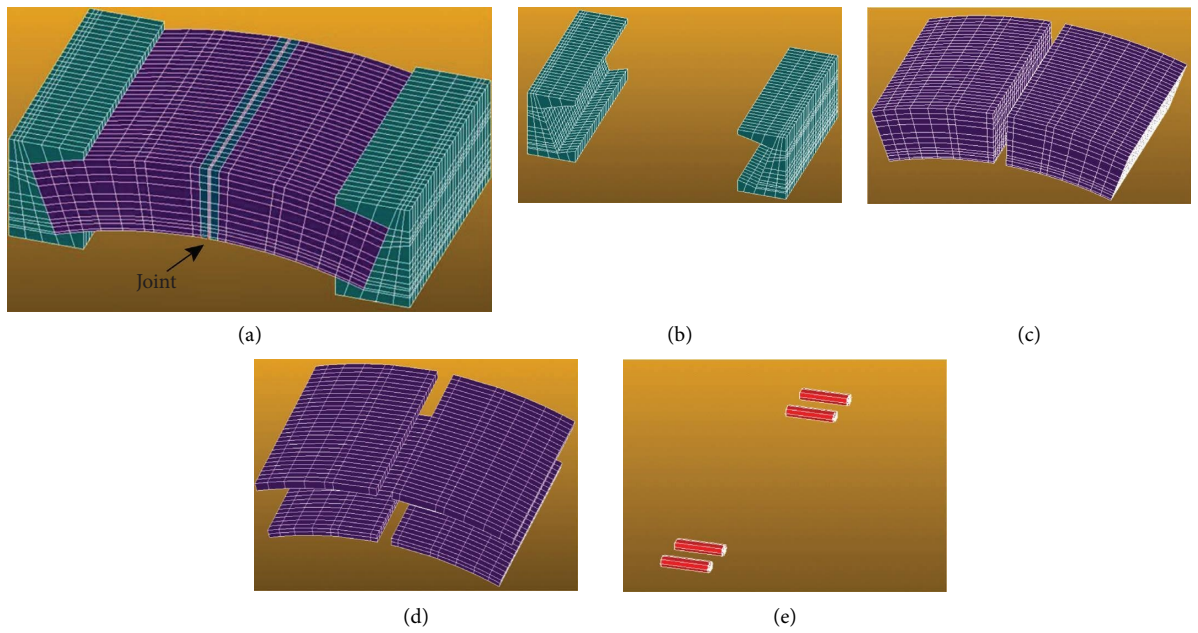

Figure 8: The finite element model for the test of segmental joints: (a) the overall numerical model; (b) the steel base; (c) the concrete segments; (d) the equivalent steel reinforcement of the segment; (e) the connecting bolts.

Table 1: The mechanical properties of the materials in the simulation.

	Young's modulus (GPa)	Poisson's ratio	Unit weight (kN·m^{-3})
Concrete	35.50	0.17	23
Steel	210.00	0.30	78
Joint	0.20	0.17	23

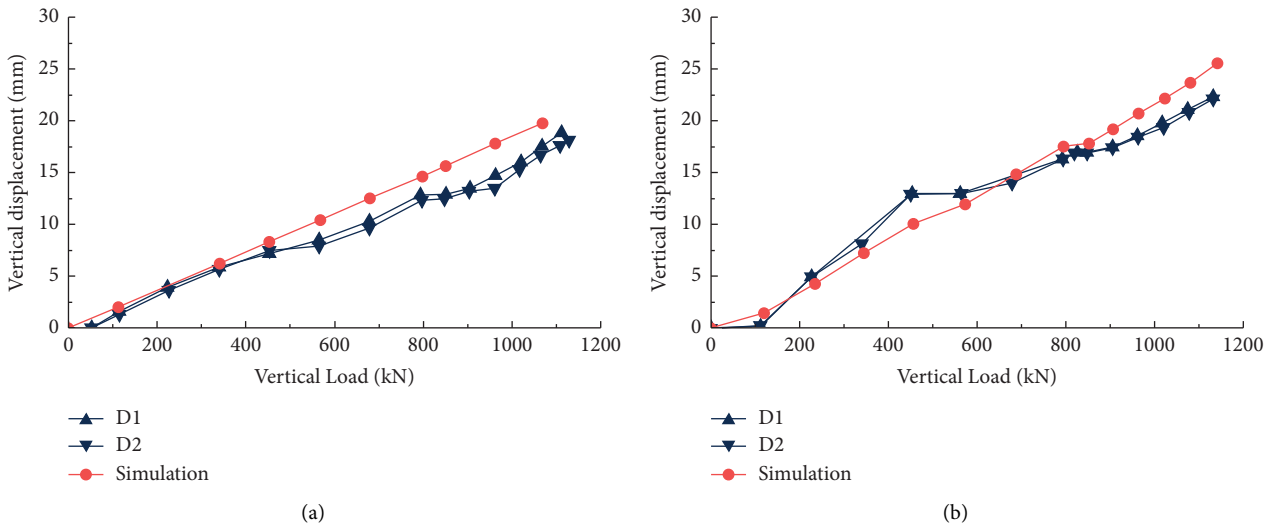

Figure 9: Continued.

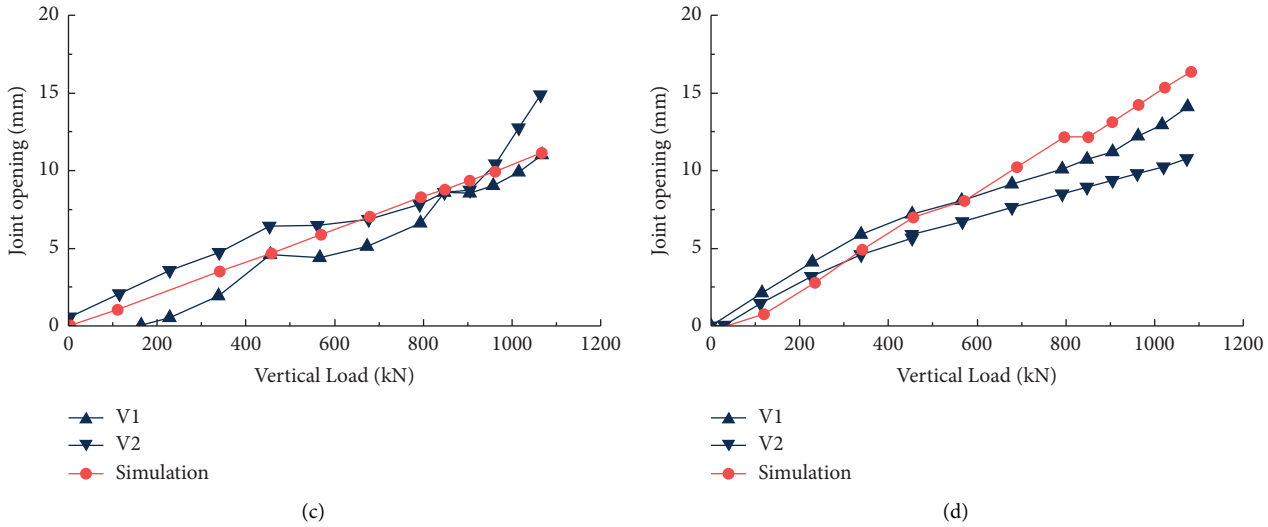

FIGURE 9: The comparison of numerical results and test results: (a) vertical displacement under positive bending moment; (b) vertical displacement under negative bending moment; (c) joint opening under positive bending moment; (d) joint opening under negative bending moment.

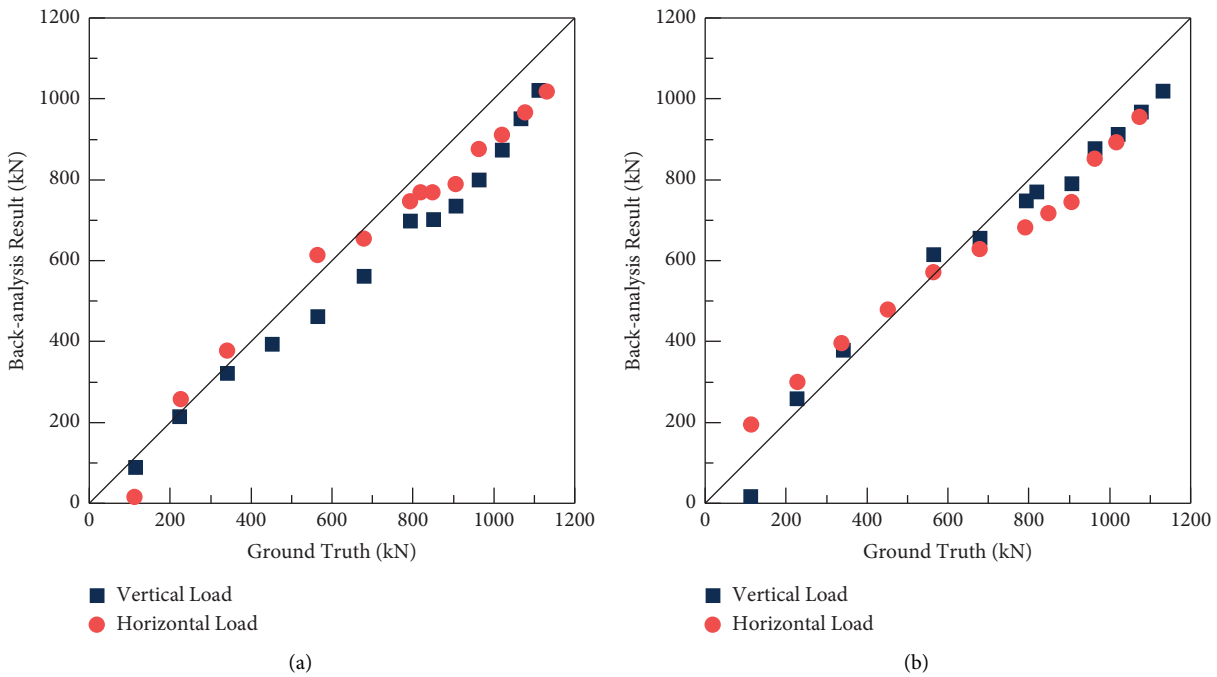

FIGURE 10: The back-analysis results of the model test: (a) positive bending moment and (b) negative bending moment.

processing are plotted in Figure 13. The irregular patterns of the loads can be found in the results, which are compatible with the scanned deformation.

4. Discussion

The proposed method provides a novel way for tunnel lining load back-analysis, without the time-consuming optimization process. Because of the irregularity in the load distribution mode, the more detailed deformation data will bring in more accurate load back-analysis results. Hence, the proposed method is suitable to be combined with laser scanning, which has the strength in acquiring a huge amount of deformation data.

The proposed back-analysis method is validated by the comparison with test results. The accurate results of back-analysis have shown promising effectiveness and feasibility. Due to the nonaccessibility of in-situ load monitoring data, the proposed method is to be applied in the practical project for further validation. The corresponding simulation model has been built to analyze the mechanical performance of the full-ring lining. For

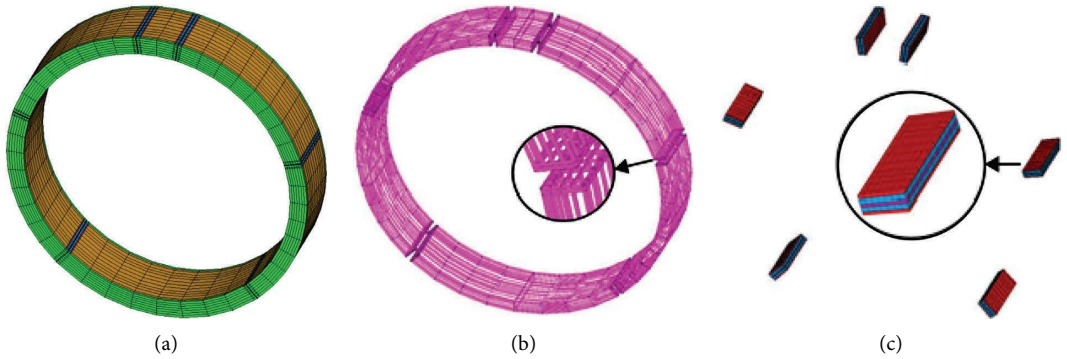

(a) (b) (c)

Figure 11: The simulation model for full-ring mechanical analysis: (a) the overall numerical model; (b) the steel reinforcement; (c) the joints.

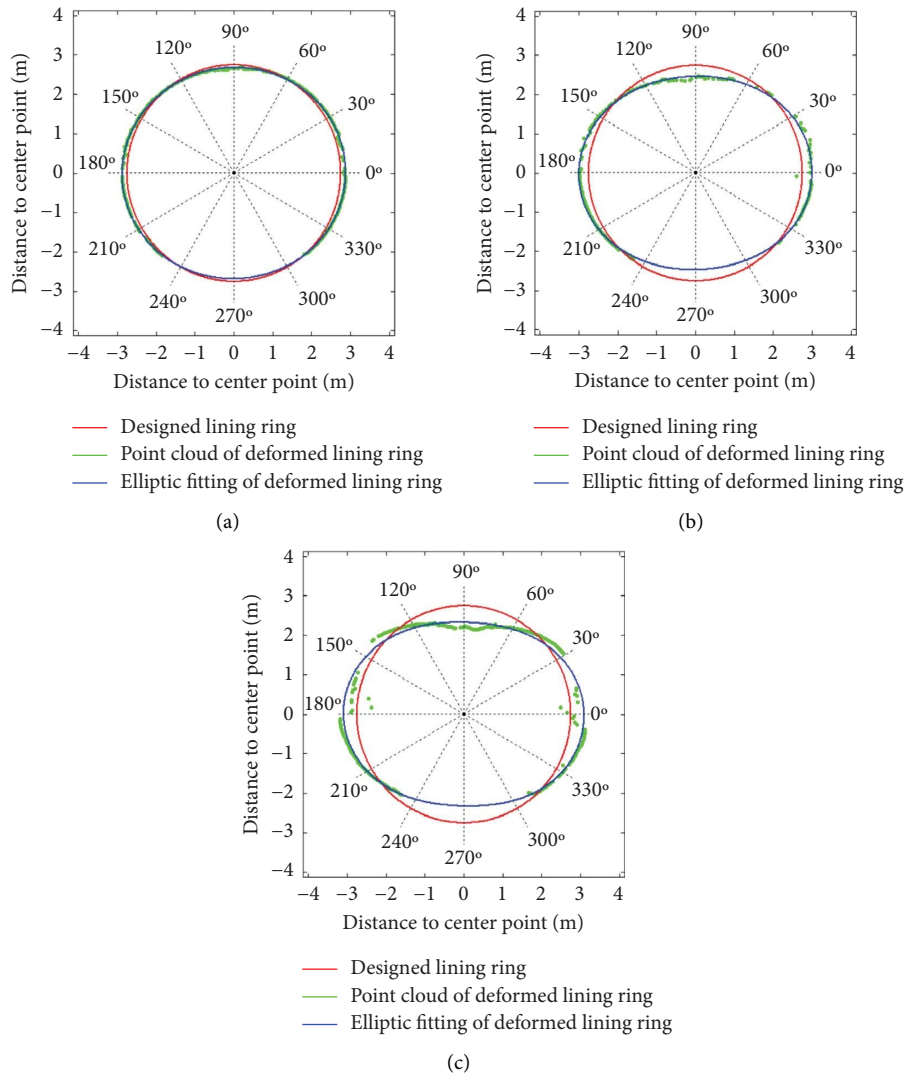

Figure 12: The deformation of the 3 lining rings: (a) ring I; (b) ring II; (c) ring III.

demonstrating the practical application of the proposed back-analysis method, the scanned full-ring deformation data are used to calculate the loads on a shield tunnel in service. The results prove that the proposed method can be used to reveal irregular load patterns, which are closer to reality. The proposed back-analysis method could be further applied in exploring the behaviour of load evolution for in-service shield tunnels.

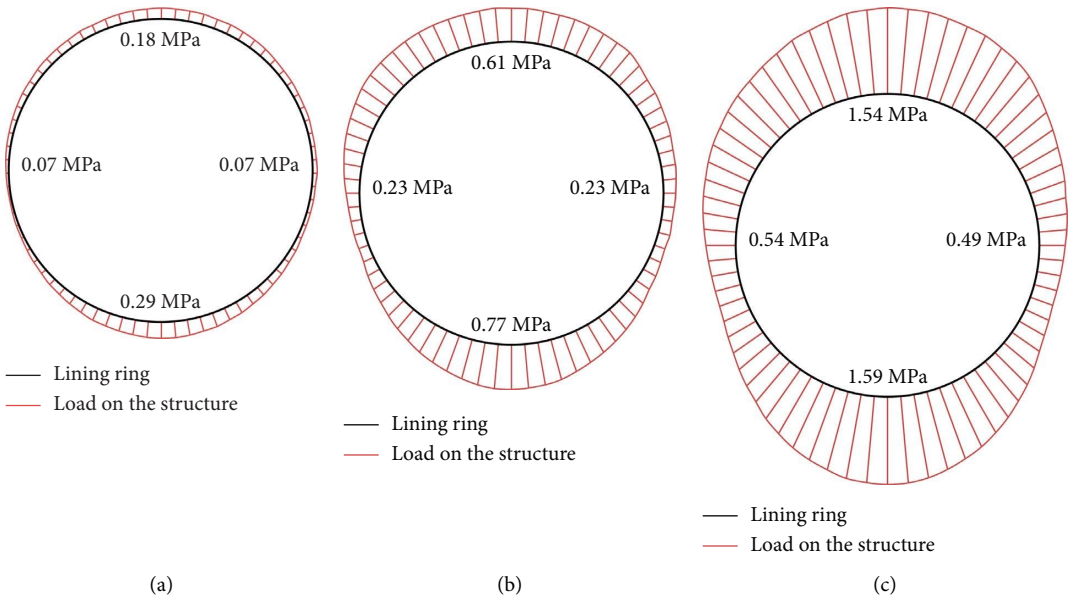

Figure 13: The back-analysis results of the 3 lining rings: (a) ring I; (b) ring II; (c) ring III.

The background of this work is in the field of shield tunnel engineering. The theory of the proposed method is not in conflict with other tunnel structures and conditions. With proper numerical modelling methods, the proposed back-analysis method can be applied to other types of tunnels, including immersed-tube tunnels. The assumption of earth pressure, however, should be carefully considered when it comes to more complicated ground situations. It is also noted that the influencing factors of deformation are more than external loads. The deformation induced by the evolution of the material and structure [55] should be further considered to pursue better accuracy.

The cost time of the proposed methods can be divided into two parts, i.e., the offline stage and the online stage. In the offline stage, plenty of simulation results will be required to establish the matrixes and equations. Hence, the cost time in the offline stage involves the time of numerical computation, which depends on the demanded accuracy and the levels of the numerical models. In the online stage, the cost time is less, which involves the calculation of equations only.

5. Conclusions

Based on Betti's theorem, the back-analysis approach is proposed in this work to study the external loads on the lining structure in the operational phase. The external load on the tunnel structure can be calculated by using the in-situ monitoring data and numerical simulations. For the in-situ monitoring, the deformation of the tunnel should be measured. According to the numerical simulation results, deformations of tunnel structure can be obtained for multiple virtual load cases. Based on the actual deformation, virtual deformation, and virtual load, the actual loads acting on the tunnel lining can be back-analyzed by using the singular value decomposition method performed by MATLAB. The proposed methods and workflows can be applied with the combination of laser scanning or other deformation measuring methods. The proposed back-analysis method allows the calculation of external loads directly instead of soil properties. The back analysis of the external loads on the lining does not involve complex optimization methods, which will minimize the computational cost of back analysis.

The data of a model test were used to verify the feasibility of the back-analysis approach. Meanwhile, the finite element model is built according to the physical model of the model test. The simulation result shows satisfying agreement with the test data. It is noted that since the rationality of the back-analyzed results depends highly on the accuracy of the numerical simulation, the model should be calibrated carefully before the load back analysis. The practical application with the scanned full-ring deformation is carried out successfully. It is indicated the back-analysis approach can be used for analyzing the loading condition on tunnel lining in operation based on the deformation data measured in practice.

Data Availability

The data used to support the findings of this study are available from the corresponding author upon request.

Conflicts of Interest

The authors declare that they have no conflicts of interest.

Acknowledgments

This work was financially supported by the National Natural Science Foundation of China (51978431 and 52038008), the Shanghai Science and Technology Development Fund

(20DZ1202004), and the State Grid Shanghai Municipal Electric Power Company Science and Technology Project (52090W220001).

References

[1] F. Stajano, N. Hoult, I. Wassell, P. Bennett, C. Middleton, and K. Soga, "Smart bridges, smart tunnels: transforming wireless sensor networks from research prototypes into robust engineering infrastructure," *Ad Hoc Networks*, vol. 8, pp. 872–888, 2010.

[2] J. Liu, C. Shi, Z. Wang, M. Lei, D. Zhao, and C. Cao, "Damage mechanism modelling of shield tunnel with longitudinal differential deformation based on elastoplastic damage model," *Tunnelling and Underground Space Technology*, vol. 113, Article ID 103952, 2021.

[3] X. Xu, S. Liu, L. Tong, and H. Li, "Reliability analysis of shield tunnel lining in service with field inspection," *Journal of Performance of Constructed Facilities*, vol. 34, no. 6, Article ID 04020111, 2020.

[4] X.-T. Lin, X. Chen, D. Su, K. Han, and M. Zhu, "An analytical model to evaluate the resilience of shield tunnel linings considering multistage disturbances and recoveries," *Tunnelling and Underground Space Technology*, vol. 127, Article ID 104581, 2022.

[5] V. E. Gall, A. Marwan, M. Smarslik, M. Obel, P. Mark, and G. Meschke, "A holistic approach for the investigation of lining response to mechanized tunneling induced construction loadings," *Underground Space*, vol. 3, no. 1, pp. 45–60, 2018.

[6] P. Chaipanna and P. Jongpradist, "3D response analysis of a shield tunnel segmental lining during construction and a parametric study using the ground-spring model," *Tunnelling and Underground Space Technology*, vol. 90, pp. 369–382, 2019.

[7] Y. Yang, B. Zhou, X. Xie, and C. Liu, "Characteristics and causes of cracking and damage of shield tunnel segmented lining in construction stage-a case study in Shanghai soft soil," *European Journal of Environmental and Civil Engineering*, vol. 22, no. sup1, pp. s213–s227, 2018.

[8] A. Jallow, C. Y. Ou, and A. Lim, "Three-dimensional numerical study of long-term settlement induced in shield tunneling," *Tunnelling and Underground Space Technology*, vol. 88, pp. 221–236, 2019.

[9] P. Lueprasert, P. Jongpradist, P. Jongpradist, and S. Suwansawat, "Numerical investigation of tunnel deformation due to adjacent loaded pile and pile-soil-tunnel interaction," *Tunnelling and Underground Space Technology*, vol. 70, pp. 166–181, 2017.

[10] R. Liang, C. Kang, L. Xiang et al., "Responses of in-service shield tunnel to overcrossing tunnelling in soft ground," *Environmental Earth Sciences*, vol. 80, no. 5, p. 183, 2021.

[11] C. Molins and O. Arnau, "Experimental and analytical study of the structural response of segmental tunnel linings based on an in situ loading test. Part 1: test configuration and execution," *Tunnelling and Underground Space Technology*, vol. 26, no. 6, pp. 764–777, 2011.

[12] E. Deng, W. Yang, X. He, Y. Ye, Z. Zhu, and A. Wang, "Transient aerodynamic performance of high-speed trains when passing through an infrastructure consisting of tunnel-bridge-tunnel under crosswind," *Tunnelling and Underground Space Technology*, vol. 102, Article ID 103440, 2020.

[13] E. Deng, X. Y. Liu, Y. Q. Ni, Y. W. Wang, and C. Y. Zhao, "A coupling analysis method of foundation soil dynamic responses induced by metro train based on PDEM and stochastic field theory," *Computers and Geotechnics*, vol. 154, Article ID 105180, 2023.

[14] K. Soga, R. G. Laver, and Z. Li, "Long-term tunnel behaviour and ground movements after tunnelling in clayey soils," *Underground Space*, vol. 2, no. 3, pp. 149–167, 2017.

[15] X. Xie, H. Tian, B. Zhou, and K. Li, "The life-cycle development and cause analysis of large diameter shield tunnel convergence in soft soil area," *Tunnelling and Underground Space Technology*, vol. 107, Article ID 103680, 2021.

[16] W. Lin, P. Li, and X. Xie, "A novel detection and assessment method for operational defects of pipe jacking tunnel based on 3D longitudinal deformation curve: a case study," *Sensors*, vol. 22, no. 19, p. 7648, 2022.

[17] O. S. Bursi, N. Tondini, M. Fassin, and A. Bonelli, "Structural monitoring for the cyclic behaviour of concrete tunnel lining sections using FBG sensors," *Structural Control and Health Monitoring*, vol. 23, no. 4, pp. 749–763, 2016.

[18] Q. Yan, W. Zhang, C. Zhang, H. Chen, Y. Dai, and H. Zhou, "Back analysis of water and earth loads on shield tunnel and structure ultimate limit state assessment: a case study," *Arabian Journal for Science and Engineering*, vol. 44, no. 5, pp. 4839–4853, 2019.

[19] P. Oreste, "Back-analysis techniques for the improvement of the understanding of rock in underground constructions," *Tunnelling and Underground Space Technology*, vol. 20, no. 1, pp. 7–21, 2005.

[20] N. Moreira, T. Miranda, M. Pinheiro et al., "Back analysis of geomechanical parameters in underground works using an evolution strategy algorithm," *Tunnelling and Underground Space Technology*, vol. 33, pp. 143–158, 2013.

[21] K. T. Kavanagh and R. W. Clough, "Finite element applications in the characterization of elastic solids," *International Journal of Solids and Structures*, vol. 7, no. 1, pp. 11–23, 1971.

[22] Q. Liu, H. Liu, X. Huang, Y. Pan, C. Luo, and H. Sang, "Inverse analysis approach to identify the loads on the external TBM shield surface and its application," *Rock Mechanics and Rock Engineering*, vol. 52, no. 9, pp. 3241–3260, 2019.

[23] C. Wu, Y. Hong, Q. Chen, and S. Karekal, "A modified optimization algorithm for back analysis of properties for coupled stress-seepage field problems," *Tunnelling and Underground Space Technology*, vol. 94, Article ID 103040, 2019.

[24] M. Mahmoudi and A. M. Rajabi, "Application of numerical back analysis for determination of soil mass specifications during tunnel construction," *Arabian Journal of Geosciences*, vol. 13, no. 19, p. 990, 2020.

[25] G. Walton and S. Sinha, "Challenges associated with numerical back analysis in rock mechanics," *Journal of Rock Mechanics and Geotechnical Engineering*, vol. 14, no. 6, pp. 2058–2071, 2022.

[26] A. Fakhimi, D. Salehi, and N. Mojtabai, "Numerical back analysis for estimation of soil parameters in the resalat tunnel project," *Tunnelling and Underground Space Technology*, vol. 19, no. 1, pp. 57–67, 2004.

[27] S. Vardakos, M. Gutierrez, and C. Xia, "Back-analysis of tunnel response from field monitoring using simulated annealing," *Rock Mechanics and Rock Engineering*, vol. 49, no. 12, pp. 4833–4852, 2016.

[28] A. Tarifard, P. Görög, and A. Torok, "Long-term assessment of creep and water effects on tunnel lining loads in weak rocks using displacement-based direct back analysis: an example from northwest of Iran," *Geomechanics and Geophysics for Geo-Energy and Geo-Resources*, vol. 8, no. 1, p. 31, 2022.

[29] W. Cai, H. Zhu, W. Liang et al., "Three-dimensional forward analysis and real-time design of deep tunneling based on digital in-situ testing," *International Journal of Mechanical Sciences*, vol. 226, Article ID 107385, 2022.

[30] R. Bertuzzi, "Back-analysing rock mass modulus from monitoring data of two tunnels in sydney, Australia," *Journal of Rock Mechanics and Geotechnical Engineering*, vol. 9, no. 5, pp. 877–891, 2017.

[31] M. Sharifzadeh, M. Sharifi, and S. M. Delbari, "Back analysis of an excavated slope failure in highly fractured rock mass: the case study of kargar slope failure (Iran)," *Environmental Earth Sciences*, vol. 60, no. 1, pp. 183–192, 2010.

[32] J. Kim, J. Kim, M. Kim, and H. Yoo, "Prediction of ground load by performing back analysis using composite support model in concrete lining design," *KSCE Journal of Civil Engineering*, vol. 19, no. 6, pp. 1697–1706, 2015.

[33] J. K. Lee, H. Yoo, H. Ban, and W.-J. Park, "Estimation of rock load of multi-arch tunnel with cracks using stress variable method," *Applied Sciences*, vol. 10, no. 9, p. 3285, 2020.

[34] H. Niu, X. Weng, C. Tian, and D. Wang, "Model test and back analysis of shield tunnel load distribution in soft clay," *Advances in Materials Science and Engineering*, vol. 2021, Article ID 9992348, 15 pages, 2021.

[35] T. Wang, B. Shi, and Y. Zhu, "Structural monitoring and performance assessment of shield tunnels during the operation period, based on distributed optical-fiber sensors," *Symmetry*, vol. 11, no. 7, p. 940, 2019.

[36] C. Zhao, A. A. Lavasan, T. Barciaga, V. Zarev, M. Datcheva, and T. Schanz, "Model validation and calibration via back analysis for mechanized tunnel simulations-the western scheldt tunnel case," *Computers and Geotechnics*, vol. 69, pp. 601–614, 2015.

[37] Y. Zhao and S.-J. Feng, "Back analysis of surrounding rock parameters of tunnel considering displacement loss and space effect," *Bulletin of Engineering Geology and the Environment*, vol. 80, no. 7, pp. 5675–5692, 2021.

[38] L. Nikakhtar, S. Zare, H. M. Nasirabad, and B. Ferdosi, "Application of ANN-PSO algorithm based on FDM numerical modelling for back analysis of EPB TBM tunneling parameters," *European Journal of Environmental and Civil Engineering*, vol. 26, no. 8, pp. 3169–3186, 2022.

[39] C. Atkinson and C. Bastero, "On the use of Betti's reciprocal theorem for computing the coefficients of stress singularities in anisotropic media," *International Journal of Engineering Science*, vol. 29, no. 6, pp. 727–741, 1991.

[40] L. Borák and P. Marcián, "Beams on elastic foundation using modified Betti's theorem," *International Journal of Mechanical Sciences*, vol. 88, pp. 17–24, 2014.

[41] R. Khandelwal and J. M. Chandra Kishen, "Thermal weight functions for Bi-material interface crack system using energy principles," *International Journal of Solids and Structures*, vol. 45, no. 24, pp. 6157–6176, 2008.

[42] L. Galuppi and G. Royer-Carfagni, "Betti's analytical method for the load sharing in double glazed units," *Composite Structures*, vol. 235, Article ID 111765, 2020.

[43] D. Nélias, E. Antaluca, V. Boucly, and S. Cretu, "A three-dimensional semianalytical model for elastic-plastic sliding contacts," *Journal of Tribology*, vol. 129, no. 4, pp. 761–771, 2007.

[44] C. Xu, B. T. Cao, Y. Yuan, and G. Meschke, "Transfer learning based physics-informed neural networks for solving inverse problems in engineering structures under different loading scenarios," *Computer Methods in Applied Mechanics and Engineering*, vol. 405, Article ID 115852, 2023.

[45] W. Zhang, X. Liu, Z. Liu et al., "Investigation of the pressure distributions around quasi-rectangular shield tunnels in soft soils with a shallow overburden: a field study," *Tunnelling and Underground Space Technology*, vol. 130, Article ID 104742, 2022.

[46] J. Chang, H. Huang, D. Zhang, H. Wu, and Y. Yan, "Transverse deformational behaviors of segmental lining during shield tunneling: A case study," *Structural Control and Health Monitoring*, vol. 29, Article ID e3097, 2022.

[47] T. Nuttens, C. Stal, H. De Backer, K. Schotte, P. Van Bogaert, and A. De Wulf, "Methodology for the ovalization monitoring of newly built circular train tunnels based on laser scanning: liefkenshoek rail link (Belgium)," *Automation in Construction*, vol. 43, pp. 1–9, 2014.

[48] X. Xie and X. Lu, "Development of a 3D modeling algorithm for tunnel deformation monitoring based on terrestrial laser scanning," *Underground Space*, vol. 2, no. 1, pp. 16–29, 2017.

[49] X. Xie, M. Zhao, J. He, and B. Zhou, "Automatic and visual processing method of non-contact monitoring for circular stormwater sewage tunnels based on LiDAR data," *Energies*, vol. 12, no. 9, p. 1599, 2019.

[50] H. Jin, S. Yu, S. Zhou, and J. Xiao, "Research on mechanics of longitudinal joint in shield tunnel by the nonlinear spring equivalent method," *KSCE Journal of Civil Engineering*, vol. 23, no. 2, pp. 902–913, 2019.

[51] W. Zhang, Q. Zhang, and W. Cao, "Study on stress and deformation of bolt joints of shield tunnel under static and seismic action," *KSCE Journal of Civil Engineering*, vol. 25, no. 8, pp. 3146–3159, 2021.

[52] H. Y. Jun and J. H. Park, "Generation of optimal correlations by simulated annealing for ill-conditioned least-squares solution," *Journal of Nuclear Science and Technology*, vol. 52, no. 5, pp. 670–674, 2015.

[53] Y. Jin, W. Ding, Z. Yan, K. Soga, and Z. Li, "Experimental investigation of the nonlinear behavior of segmental joints in a water-conveyance tunnel," *Tunnelling and Underground Space Technology*, vol. 68, pp. 153–166, 2017.

[54] S. G. Lorenzo, "The role of temporary spear bolts in gasketed longitudinal joints of concrete segmental linings," *Tunnelling and Underground Space Technology*, vol. 105, Article ID 103576, 2020.

[55] M. O. Ahmed, R. Khalef, G. G. Ali, and I. H. El-adaway, "Evaluating deterioration of tunnels using computational machine learning algorithms," *Journal of Construction Engineering and Management*, vol. 147, no. 10, Article ID 04021125, 2021.